Pharm Res (2018) 35: 167
https://doi.org/10.1007/s11095-018-2451-0

RESEARCH PAPER

Continuous Single-Step Wet Granulation with Integrated in-Barrel-Drying

Adrian Schmidt [1,2] • Hans de Waard [2] • Peter Kleinebudde [1] • Markus Krumme [2]

Received: 5 February 2018 / Accepted: 18 June 2018 / Published online: 25 June 2018

ABSTRACT

Purpose It was investigated if continuous wet granulation and drying could be combined in a twin-screw granulator with the aim to provide (pre-)dried granules in a single-step process, i.e. in-barrel-drying.

Methods To have a consistent and robust material propulsion mechanism, a twin-screw granulator was divided into two compartments. One compartment was operated at lower temperature to granulate and to pre-heat the material, while another compartment was operated at very high temperature to evaporate the granulation liquid as rapidly as possible. Design of experiments was used to investigate the in-barrel-drying process in detail. The process was further investigated for twin-screw wet granulation with API suspension feed, and compared against traditional fluidised-bed drying. Granule and compact properties were evaluated to study the process impact on the product quality.

Results In-barrel-drying was demonstrated as feasible and yielded completely dried and granulated material at specific settings. The evaporation zone temperature and the processed mass of water were identified as key parameters to balance the evaporation capacity of the process and the material throughput. Granules and compacts showed an acceptable product quality.

Conclusions In-barrel-drying can be used to condense the wet granulation and drying process steps into one piece of equipment, thereby limiting or even omitting downstream drying process steps.

✉ Markus Krumme
Markus.Krumme@novartis.com

[1] Institute of Pharmaceutics and Biopharmaceutics, Heinrich-Heine-University, 40225 Duesseldorf, Germany

[2] Novartis AG, WSJ-027.4.015, Novartis Campus, 4002 Basel, Switzerland

KEY WORDS API suspension feed · design of experiments · fluidised-bed drying · telescoped process · twin-screw wet granulation

ABBREVIATIONS

API	Active pharmaceutical ingredient
CP	Centre point
DOE	Design of experiments
HPLC	High performance liquid chromatography
L/S ratio	Liquid-to-solid mass flow ratio
LOD	Loss-on-drying
ScSp	Screw speed
Temp.Eva	Temperature in the evaporation zone
Temp.Pre	Temperature in the pre-heating zone
TMMF	Total material mass flow rate
TSG	Twin-screw granulator

INTRODUCTION

In pharmaceutical manufacturing of drug product, wet granulation is a commonly used technique to enlarge the particle size of powders (1,2). Thereby, powder blend properties, such as flowability, density and/or segregation behaviour, are improved for downstream processing (e.g. tableting) (3). In wet granulation, a granulation liquid (typically water) is added to the powder blend to form nuclei followed by particle agglomeration (4). However, since the typical quantity of water used are detrimental for further process steps (e.g. sticking to punch surfaces during tableting) and the final drug product quality, the granulation liquid has to be removed again during the next process step (5,6). Consequently, a wet granulation process is followed by a drying operation.

In continuous manufacturing of drug product, one way to implement wet granulation and drying in the manufacturing line is by using twin-screw wet granulation and fluidised-bed drying technology (7). Specifically the twin-screw granulator (TSG) offers a high versatility in its applications (8). Besides the variable screw design that can be utilised to manipulate granule properties, the TSG combines multiple unit operations in one piece of equipment, namely blending, wet granulation and/or sizing (9,10).

Another feature of the TSG was shown in the link of chemical (primary) and pharmaceutical (secondary) continuous manufacturing. A fully integrated end-to-end continuous manufacturing process, including a wet granulation unit operation, was claimed to be achieved by using API suspension feed in twin-screw wet granulation (Schmidt A, de Waard H, Moll K-P, Kleinebudde P, Krumme M; Simplified end-to-end continuous manufacturing by feeding API suspensions in twin-screw wet granulation. 2018. Submitted for publication). In this example, the API suspension (typically obtained after the upstream unit operations API crystallisation and washing) was dosed directly into the TSG. Previously required API drying and milling steps were omitted as the suspending liquid was used directly as granulation liquid. The suspension feed thereby represented the interface between continuous manufacturing of drug substance and continuous manufacture of drug product. As the drug substance has already been crystallized in the envisioned setup and as long as the API is practically insoluble in the aqueous suspending liquid, the risk of formation of a different polymorph is minimal.

However, it was shown that new challenges need to be addressed when using API suspension feed. For such a process setup, the dosed amount of API and water are linked. Consequently, the amount of water in the process cannot be freely chosen. To a certain extent, the API suspension concentration could be de−/increased to tailor the quantity of water in the process. However, this approach is limited since the rheological behaviour changes significantly upon increasing the API load in the suspension and may affect the processability. Especially when highly drug-loaded formulations are targeted, large quantities of water can challenge the process boundary in wet granulation. From a wet granulation processing point of view, this challenge could be addressed by development of a suitable formulation (4). However, as a consequence of omitting previous drying steps and the use of the original solvent for granulation, more extensive drying was required after wet granulation.

In this study, it was hypothesised that the versatility of the TSG could be extended even further by utilising it for drying of wet granules. In literature, screw conveyors have been described as pre-dryer and/or post-dryer (11,12). The considerable advantage of a screw conveyor dryer is the true continuous process principle, the firmly controlled material throughput and its compact design and cost efficiency. The TSG, as a type of screw conveyor, provides the function of individual segmented temperature control of barrel zones. It was assumed that by heating certain parts of the equipment, wet granulation and (pre-) drying could be combined inside the barrels, from now on referred to as in-barrel-drying.

Although in a different context and with a completely different scope, a study has indicated the possibility of receiving dried granules after twin-screw wet granulation at higher temperatures (13). The aim was to enhance the tabletability of a poorly compactible drug, using twin-screw wet granulation at barrel zone temperatures up to 90°C. Since only a very low amount of water (5%) was processed, dried granules were obtained for specific settings.

However, the objective in this study was to specifically focus on investigating the drying capability by in-barrel-drying in a TSG (by use of barrel temperatures up to 220°C). In the first part of this study, the impact of several process parameters on the in-barrel-drying was investigated in detail by using design of experiments (DOE). In a screening DOE, favourable factor ranges and combinations have been identified for receiving (pre-) dried granules. In the second part of this study, the identified ranges and combinations were further investigated in an optimisation DOE, to improve modelling and the predictive power. In the final part of this study, the previously developed API suspension feed was combined with the in-barrel-drying process. Granules (particle size distribution, bulk/tapped density) and compact properties (tensile strength, out-of-die porosity, disintegration time) were studied and compared against traditional fluidised-bed drying.

MATERIALS AND METHODS

Materials

Lumefantrine was used as a model drug substance (Zhejiang Medicine Co., Zhejiang, China). Other materials in this study were lactose monohydrate (lactose spray dried, Kerry Bio-Science, Norwich, USA), microcrystalline cellulose (Vivapur® 102, JRS Pharma, Rosenberg, Germany), sodium carboxymethylcellulose (Primellose®, DFE Pharma, Goch, Germany), polyvinylpyrrolidone K30 (Plasdone® K-29/32, Ashland, Covington, USA) and magnesium stearate (magnesium stearate Eur.Pharm., Faci, Carasco, Italy). In the case of the lumefantrine suspension feed, polysorbate 80 (Tween® 80, Croda International, Snaith, UK) was used as suspension aid. Demineralised water was used as granulation liquid (respectively suspending liquid).

Preparation of Granulation Powder Blends

Lumefantrine was sieved manually through a 1 mm mesh before use. Powder blends were dispensed for a single mixing

step in batch sizes ranging between 2 and 4 kg (Table I). The mixing drum was filled up to a volume of approximately 75% and blended, using a turbula blender (type T10A, Willy A. Bachofen, Muttenz, Switzerland) for 5 min at 25 rpm. After blending, powder blends were sieved again manually (1 mm).

Preparation of Granulation Fluid

For the characterisation of the in-barrel-drying process, only demineralised water was used as granulation fluid. For the comparison of in-barrel-drying against fluidised-bed drying, a lumefantrine suspension was used as granulation fluid. Lumefantrine is practically insoluble in the aqueous granulation liquid. Therefore, polymorphic effects were excluded when working with API suspension feed. Polysorbate 80 was dissolved in demineralised water to aid the wetting and thereby the suspending of lumefantrine. The lumefantrine was sieved manually through a 1 mm mesh, before it was added in small portions (approximately 25 g every 5 min) until the targeted suspension concentration was achieved. The lumefantrine concentration in the suspension was 25% *w/w*. The suspension was manufactured in batch sizes of 400 g.

Twin-Screw Wet Granulation

A co-rotating Pharma 11 mm TSG (Thermo Scientific Pharma 11, Thermo Fisher Scientific, Karlsruhe, Germany) was used, equipped with screws (screw diameter (D): 11 mm; screw length: 40 ¾ D) in the configuration 1 D conveying element (CE), 4 D long helix CE, 18 D CE, 1 ½ D kneading elements at 60° staggering angle, 1 D CE, 1 ¼ D kneading elements at 30°staggering angle, 10 D CE and 4 D distributive flow elements (Fig. 1). Further, the TSG was divided into two different temperature zones. Barrel zones 2 to 5 were defined as "pre-heating" zone, whereas barrel zones 6 to 8 were defined as "evaporation" zone. Barrel zone 1 could not be temperature controlled. The TSG was equilibrated for at least 45 min at start-up, until the heating performance stabilised and before experiments were started whenever temperature settings were changed. For cooling, a chiller (Thermo Scientific NesLab Thermoflex 1400, Thermo Fisher Scientific, Karlsruhe, Germany) was used with water cooled to 15°C. The moisture vapour was vented from the TSG via the natural opening towards the end of the screws. All process parameters have been monitored throughout the process, using the data logging software provided by Thermo Fisher. The powder blend was dosed to the TSG (barrel zone 1), using a Brabender gravimetric feeder (DDW-MD0-MT-1, Brabender, Duisburg, Germany). The granulation fluid was dosed to the TSG (barrel zone 2), using either a HPLC pump (Smartline pump 100, Knauer, Berlin, Germany) or a progressing cavity pump (NM003BY11S12B, Netzsch, Selb, Germany).

Characterising in-Barrel-Drying by Using Design of Experiments

In general, drying processes are impacted significantly by the heat-transfer, which in turn is affected (in the case of contact dryers such as screw conveyers) by the contact surface area between material and heat source (e.g. the barrel), the temperature difference between material and heat source, as well as the material residence time (=drying time). Therefore, five factors were selected: the total material mass flow rate, the L/S ratio, the screw speed, and the temperatures in the pre-heating and in the evaporation zone. The total material mass flow rate was selected to define the material throughput per time and is provided by the sum of the solid feed and the liquid feed. Thereby, the total material mass flow rate impacts the TSG fill-level and hence the contact surface area between material and barrel. Additionally, it impacts the water quantity in the process. The L/S ratio was selected to define the material composition. It impacts the water quantity in the process. The screw speed was selected to define the material transport in the TSG and to give control over the material residence time (drying time) (14). Finally, the pre-heating and evaporation zone temperature were selected to control the barrel temperature in the different compartments of the equipment and thereby the temperature difference between material and barrel. Other surrogated parameter like the

Table I Final Formulation Composition

Compound	Characterisation of in-barrel-drying [% *w/w*]	Comparison in-barrel-drying and fluidised-bed drying [% *w/w*]
Lumefantrine	20.0	20.0
Lactose spray dried	35.0	35.0
Microcrystalline Cellulose	33.5	33.0
Sodium carboxymethylcellulose	6.0	6.0
Polyvinylpyrrolidone K30	4.0	4.0
Magnesium stearate	1.5	1.5
Polysorbate 80	–	0.5

Underlined components were processed via the granulation liquid, others in a powder blend

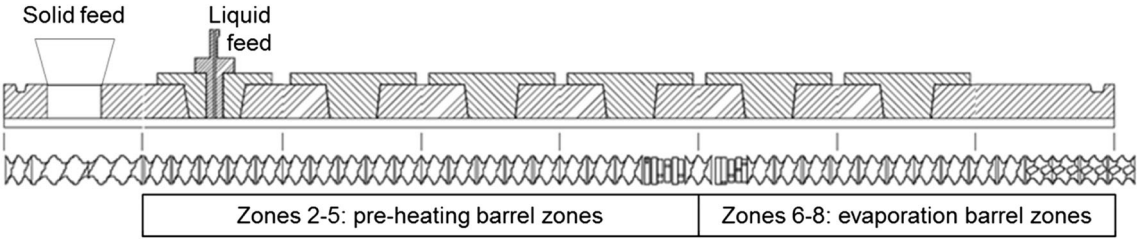

Fig. 1 Setup of the screw configuration and the barrel temperature zones.

specific fill-load for the fill-level (=total material mass flow rate divided by the screw speed) (15) were considered but not selected for this investigation, since those cannot be controlled individually and may combine too many effects. For example, the specific fill-load may confound effects from liquid feed, solid feed and/or screw speed.

For the first (screening) DOE, a 29-run fractional factorial three-level central composite face-centred design (2^{5-1}) has been selected. Factors were investigated in the ranges: 240–500 g/h (total material mass flow rate), 0.6–1.0 (L/S ratio), 50–350 rpm (screw speed), 20–100°C (pre-heating zone temperature) and 160–200°C (evaporation zone temperature). For the second (optimisation) DOE, a 31-run fractional factorial five-level central composite circumscribed design (2^{5-1}) has been selected. The design included an additional single experiment in the corner of highest temperatures in the barrel zones and lowest total material mass flow rate, L/S ratio and screw speed. Factors were investigated in the ranges: 360–560 g/h (total material mass flow rate), 0.6–0.8 (L/S ratio), 50–100 rpm (screw speed), 60–100°C (pre-heating zone temperature) and 205–215°C (evaporation zone temperature). The factors were coded as −1 (lower level), 0 (centre point level) and + 1 (upper level).

For every experiment, in-barrel-drying was performed over a process run time of 20 min after which, the product temperature was assessed on granules at different locations, directly after the material exited the TSG. A contact thermometer was used (Thermocouple Traceable®, VWR, Radnor, USA). Only the highest and therefore most critical product temperature for material degradation was taken into account for further evaluation. Between 17 and 20 min process run time, granules were collected for LOD analysis. The product LOD was measured using a moisture analyser (HS153, Mettler Toledo, Greifensee, Switzerland). A sample of 5–6 g was dried at 105°C temperature, until the loss in weight was less than 1 mg over 50 s. Furthermore, the product LOD was used to calculate the evaporated mass of water per unit of time (= introduced mass of water by solid and liquid feed minus residual mass of water in the product) and the drying efficiency (= evaporated mass of water divided by introduced mass of water by liquid feed). The dried granules from the LOD analysis were measured for their particle size distribution using a Camsizer XT (Camsizer XT, Retsch Technology, Haan, Germany) equipped with an air-jet module. The air dispersion pressure was set to 30 kPa. The particle size was measured based on the smallest of all maximum chord lengths of the particle projections (inner width). A volume based particle size distribution was determined and the median particle size (x_{50}) was calculated.

Another very important material attribute is the material density of incoming and resultant material. The incoming material density is of importance for the mechanism by which the contact surface area with the barrel is affected. However, the material density changes continuously along the granulation process (e.g. by the impact of shear forces) before reaching the evaporation zone. The resultant material density is of importance as a property for downstream processes (e.g. tableting). However, this property is affected significantly by the setup of the final manufacturing process (e.g. additional drying or milling steps). Since this study aims to show a proof of concept for combining granulation and drying in a TSG, the material density was not included in the study design. However, when a final manufacturing process has been defined, the resultant material density has to be considered for the design.

Using multiple linear regression, a model was fitted. The response distribution was checked. Further, it was determined if data transformation is needed. The model was refined using backward regression of non-significant terms. Every model was checked for model quality based on 4 quality parameters: goodness of fit (R^2), goodness of prediction (Q^2), model validity and reproducibility. The R^2 displays how well the model explains the obtained response variation. The Q^2 gives an estimate of the predictive power of the model. The model validity and reproducibility give a measure for the lack of fit of the model and the pure error. The best model quality is represented by a value of 1. However, the acceptance criteria for the model were set according to recommendations given in literature (16): R^2 and Q^2 must be higher than 0.5 and the difference between the two smaller than 0.2–0.3; the model validity must be higher than 0.25 to indicate a sufficiently low model error (the *p*-value was set to 0.05); the reproducibility must be higher than 0.5. The resulting values of the coefficients were normalised over all process responses.

All experiments were designed and evaluated using the DOE software MODDE (MODDE 11.0.1, Sartorius-stedim, Aubagne, France).

Comparison of in-Barrel-Drying and Fluidised-Bed Drying

Granulation and Drying

For in-barrel-drying, the following parameters were selected: the total material mass flow rate was 360 g/h, the L/S ratio was 0.6, the screw speed was 50 rpm, the pre-heating zone temperature was 100°C and the evaporation zone temperature was 215°C. If needed, the screw speed was adapted slightly (+ 7 / − 5 rpm), in order to control the product LOD in narrow ranges while keeping the product temperature below the melting point of lumefantrine (128°C). If the drying efficiency of the process was too high, the product temperature increased rapidly, hence the screw speed was increased slightly (resulting in a decrease in residence time and hence drying time and drying efficiency). If the drying efficiency of the process was too low, the screw speed was decreased (similarly, increase in drying time and drying efficiency). The process was operated over a process run time of 140 min, in order to collect a sufficient amount of granules for the following compaction unit operation. At time points 20, 50, 80, 110 and 140 min, granules were collected to verify the product LOD. The product temperature was measured at least every 10 min.

For fluidised-bed drying, the total material mass flow rate, as well as the L/S ratio were kept constant. The screw speed was set to 47 rpm and the barrel temperature to 20°C in all barrel zones. The process was operated over a process run time of 140 min. Granules were collected between 20 and 140 min process run time. At the time points 20 and 140 min, samples were collected to verify the product LOD. Granules from 20 to 50 min, 50 to 80 min, 80 to 110 min and 110 to 140 min process run time were defined as sub-batch and dried using a fluidised-bed dryer (Mini Glatt 5, Glatt, Binzen, Germany). The fluidised-bed dryer was pre-heated initially for at least 1 h. The equipment was equilibrated at an exhaust air temperature of approximately 40°C. Then, the material was loaded into the equipment and the air flow was increased until proper fluidisation of the wet granules was observed (the pressure drop was approximately 0.1 bar). The granules were dried at an inlet air temperature of 65°C (inlet air humidity varied from 21 to 38% and was measured at 21°C (room conditions)). To remove fines from the filters during processing and to prevent any clogging, they were blown-out by compressed air every 5 s for a duration of 0.5 s. When the exhaust air temperature approached values around 40°C, the drying process was interrupted and the product LOD was checked. If the product LOD of the granules was comparable to the LOD of the original powder blend, the drying was stopped. If not, drying was continued. The process run time was approximately 30 min. In order to collect most of the fines, the filters were blown-out by compressed air every 1 s (duration 0.5 s) over 1 min, before the material was finally discharged from the dryer. The fluidised-bed drying process was not optimised and kept constant at the listed parameters, since the focus of this study was on in-barrel-drying.

Granule Properties

The true density was determined from granules that were stored in a desiccator at room temperature and a relative humidity of 43 ± 1% (saturated potassium carbonate solution) for approximately 48 h, using a helium pycnometer (AccuPyc 1340 V2.0, Micromeritics, Norcross, USA). All measurements were conducted in triplicate (5 purging runs, 34.5 Pa/min equilibration rate, 2.0 g sample size). The bulk and tapped density were measured as described in the European Pharmacopoeia (Eur.Ph.), using a 250 ml measuring cylinder (graduated to 2 ml) and a tapped density tester (STAV 2003, J.Engelsmann, Ludwigshafen, Germany). A comparison of the granule morphology was performed based on imaging using a scanning electron microscope (SUPRA 40, Carl Zeiss, Oberkochen, Germany).

Compaction and Compact Properties

Dried granules were sieved manually (1 mm mesh) before compaction. 500 mg round flat face compacts were manufactured (diameter 11.28 mm). A fully instrumented compaction simulator (Stylcam® 200R, Medelpharm, Beynost, France) was used to mimic a FETTE P1200. The dwell time of 13 ms was kept constant, whereas the compaction pressure was varied (50, 100, 150, 200, 250 and 300 MPa). For each compaction pressure, 10 compacts were manufactured (for analyses of compact height and breaking force). At 100 MPa, another 25 compacts were produced for the analyses of friability and disintegration time.

The compact height was measured immediately after compaction by using a calliper (Traceable®, VWR, Radnor, USA). The out-of-die porosity has been calculated using the compact height and diameter (punch diameter) and the true density of the granules. The tensile strength has been calculated from the compact dimensions and the breaking force (Pharmatron MultiTest 50, Pharmatron, Thun, Switzerland). The friability (AE-1, Charles Ischi, Zuchwil, Switzerland) (1 run) and the disintegration time (Pharmatron DisiTest 50, Pharmatron, Thun, Switzerland) (6 compacts) have been measured as described in the Eur.Ph. (friability 2.9.7; disintegration time 2.9.1) on compacts manufactured at 100 MPa.

RESULTS AND DISCUSSION

Screening DOE

In this feasibility study, it was investigated whether wet granulation and drying could be combined in a TSG (proof of concept). First, a screening DOE was selected to identify critical process parameters and their appropriate ranges. A broad knowledge space was targeted (i.e. relatively wide factor ranges were chosen; (Table II)). The process responses were shown to be sensitive to the investigated factor ranges. After model refinement, models were obtained that were descriptive, predictive, significant and reproducible for all process responses (Table III). Models of the product LOD, the evaporated mass of water and the drying efficiency showed a high descriptive and predictive power, whereas models of product temperature and granule size x_{50} were shown to be valid and applicable, at least for indicating trends, but with less descriptive and predictive power. For the product temperature, this could be attributed to the applied measurement method (e.g. the product temperature decreased rapidly after the material exited the granulator). For the model of the granule size x_{50}, the lower descriptive and predictive power could be explained by the lower reproducibility, which in turn could be attributed to the high temperatures in the granulator. Higher pre-heating zone temperatures could have impacted the particle agglomeration by the evaporation of at least some of the granulation liquid. Furthermore, mechanical and/or other stresses (caused by rapid heating and water evaporation) could have caused granule breakage in the evaporation zone. The obtained bimodal particle size distribution could be an indication for granule breakage. Both increase experimental variability and reduce the reproducibility. However, for all process responses, statistically significant models were implemented successfully to analyse the effects of investigated factors.

In particular, the process response "product LOD" but also the "granule size x_{50}" were considered crucial since these indicate successful (pre-) drying and granule formation, respectively. For the product LOD, main effects of all investigated factors were obtained (Fig. 2a). In general, all effects can be explained by the principles of heat-transfer and heat-requirements for the water evaporation. E.g. the heat-transfer increases when the temperature difference between the material and the barrel surface is increased (17). Consequently, the water evaporation is emphasised and the product LOD decreases (main effects of the pre-heating zone and the evaporation zone temperature). In contrast, the heat-transfer decreases when the material residence time is decreased significantly (main effect of the screw speed; interaction effect of the screw speed and the evaporation zone temperature) (18). Thereby the drying time is shortened, less water is evaporated and hence the product LOD increases. Moreover, the product LOD increases, when the heat-requirements for the water evaporation are increased significantly (main effects of the L/S ratio and the total material mass flow rate; interaction effect of the total material mass flow rate and the pre-heating zone temperature).

Obtained effects are getting more complex, if both, the heat-transfer and the heat-requirements for the water evaporation are affected in parallel. E.g. the product LOD increases rapidly by increasing the L/S ratio or the screw speed. However, the gradient of the function (product LOD as function of the L/S ratio and the screw speed respectively) decreases constantly at higher ranges of these factors (square effects) (Fig. 2b). By increasing the L/S ratio, the heat-requirements for the water evaporation increase rapidly (increasing water quantity). However, this effect is hypothesised to be increasingly compensated by a simultaneous increase in the heat-transfer (increase in the contact surface between material and barrel since the liquid density is higher than the density of a bulk powder; and the thermal conductivity for stainless steel is higher than for air (19,20)). By increasing the screw speed, the heat-transfer decreases significantly by decreasing the material residence time (drying time). However, this effect is hypothesised to be increasingly compensated by a simultaneous decreasing TSG fill-level, which in turn results in a more favourable ratio between the material volume and the material contact surface with the barrel.

For the granule size x_{50}, main effects were obtained for the factors L/S ratio and pre-heating zone temperature (Fig. 2c). The L/S ratio is one of the most crucial process parameter for inducing particle agglomeration in twin-screw wet granulation (21). Therefore, it is obvious that increasing L/S ratios increase the granule size x_{50}. However, the pre-heating zone temperature triggers the evaporation, at least of some of the water, leading to a lower L/S ratio in the process and hence decreases the granule size x_{50}. This explanation is supported by the obtained interaction effect between the L/S ratio and the pre-heating zone temperature.

Furthermore, an interaction effect was obtained between the total material mass flow rate and the screw speed (Fig. 2d). By increasing the total material mass flow rate at high screw speed, the granule size x_{50} was increasing. However, doing the similar at low screw speed resulted in a decrease of the granule size x_{50}. In both cases, the TSG fill-level increases by increasing the total material mass flow rate. Furthermore, the TSG fill-level is higher at low screw speed, compared to high screw speed (constant total material mass flow rate). According to literature, the fraction of coarse particles increases by increasing the TSG fill-level (15). The described effect of the TSG fill-level was studied with a screw design using a single distributive flow element, directly after the kneading zones. Therefore, granules would be expected even coarser at low screw speed than at process settings with high screw speed. However, in the current study a screw design was selected including four

Table II Factor Settings and Obtained Process Responses for the Screening DOE

	Factors					Responses				
Exp. Range	TMMF [g/h] 240–500	L/S ratio 0.6–1.0	ScSp [rpm] 50–350	Temp. Pre [°C] 20–100	Temp. Eva [°C] 160–200	ProductLOD [*w/w* %] 3.2–35.4	Evapor. mass H_2O [g/h] 59–198	x_{50} [μm] 169–456	Product temp. [°C] 58–89	Drying efficiency [%] 45–97
1	500	1.0	350	20	160	35.4	121	423	59	45
2	240	0.6	350	20	160	19.1	59	308	62	61
3	240	1.0	50	20	160	27.5	78	467	58	62
4	500	0.6	50	20	160	23.9	98	253	63	48
5	370	0.8	200	60	160	29.6	84	413	64	47
6	240	1.0	350	100	160	24.1	85	274	63	68
7	500	1.0	50	100	160	30.5	148	167	70	56
8	500	0.6	350	100	160	22.4	106	350	66	52
9	240	0.6	50	100	160	12.2	73	333	63	77
10	370	0.8	200	20	180	24.9	102	445	68	58
11 CP	370	0.8	200	60	180	24.4	104	317	67	63
12 CP	370	0.8	200	60	180	25.4	101	283	66	58
13 CP	370	0.8	200	60	180	25.7	99	385	63	57
14	240	0.8	200	60	180	20.9	75	394	63	67
15	500	0.8	200	60	180	28.2	122	456	66	51
16	370	0.6	200	60	180	17.7	95	352	64	64
17	370	1.0	200	60	180	28.1	118	383	64	61
18	370	0.8	50	60	180	19.6	120	393	59	70
19	370	0.8	350	60	180	23.9	106	418	62	61
20	370	0.8	200	100	180	22.6	110	445	64	64
21	240	0.6	50	20	200	3.2	88	325	89	95
22	500	1.0	50	20	200	20.5	198	372	65	74
23	500	0.6	350	20	200	20.0	118	348	72	58
24	240	1.0	350	20	200	22.3	89	397	60	71
25	370	0.8	200	60	200	20.7	116	412	64	67
26	500	0.6	50	100	200	7.5	170	273	85	91
27	240	1.0	50	100	200	4.9	117	297	84	97
28	240	0.6	350	100	200	6.2	84	169	88	93
29	500	1.0	350	100	200	24.4	176	308	64	71

TMMF total material mass flow rate [g/h], *L/S ratio* liquid-to-solid mass flow ratio, *ScSp* screw speed [rpm], *Temp. Pre* temperature in the pre-heating zone [°C], *Temp. Eva* temperature in the evaporation zone [°C], *CP* centre point

Table III Summary of Model Fit for the Screening DOE after Model Refinement

Process response	Goodness of fit (R^2)	Goodness of prediction (Q^2)	Model validity	Reproducibility
Quality parameters	> 0.50	> 0.50	> 0.25	> 0.50
Product LOD	0.99	0.97	0.70	0.99
Evaporated mass H_2O	0.99	0.96	0.67	0.99
Drying efficiency	0.98	0.95	0.95	0.95
Ganule size x_{50}	0.76	0.54	0.84	0.75
Product temp.	0.81	0.60	0.57	0.94

distributive flow elements at the screw end. In literature, distributive flow elements were reported to introduce milling effects (10). It is hypothesised, that granules were indeed coarser initially at low screw speed (compared to high screw speed). However, the interim coarser granules triggered intensive milling in the zone of distributive flow elements, leading to an overall decrease in the granule size x_{50}. Contributing factors for the granule breakage could have been stresses of very high temperatures and rapid water evaporation. This explanation could be supported by the obtained square effect for the L/S ratio.

The objective of achieving particle agglomeration and a low product LOD simultaneously raised challenges. E.g. certain water quantities are required to initiate particle agglomeration (22) but it should also be noted that increasing the amount of water may decrease the drying efficiency and hence increase the resulting product LOD (4). The described situation was reflected in the pareto plots of the two process responses (Fig. 2a and c). The majority of the main and square effects, which were shown to be beneficial for increasing the granule size x_{50}, simultaneously increased the product LOD (main effects of the L/S ratio and the pre-heating zone temperature, square effect of the L/S ratio). Only the evaporation zone temperature was shown to be beneficial to achieve dry granules, while still ensuring particle agglomeration. This indicates, that after granules were formed in the first compartment of the TSG (pre-heating zone), the temperature was no longer relevant for their size in the evaporation zone. This

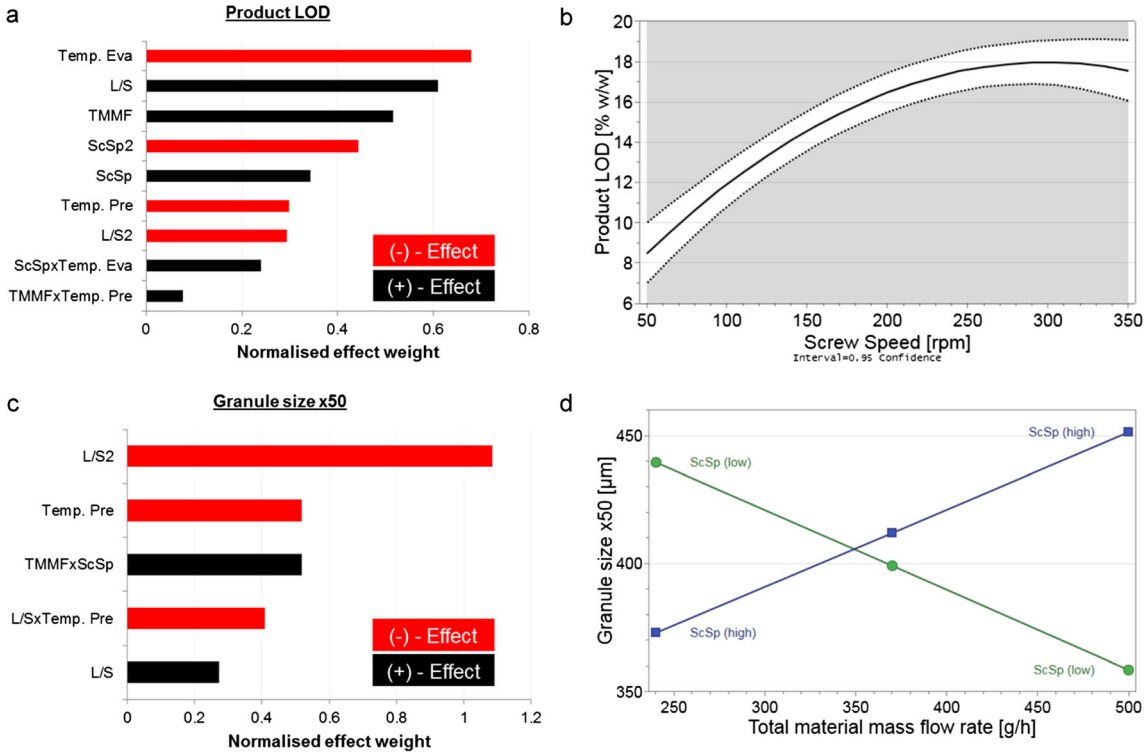

Fig. 2 (**a**) Pareto plot of significant effects on the process response product LOD. A minus/plus main effect of a factor thereby represents a decrease/increase in the process response, when the factor is increased from its low level to its high level, while the other factors remain constant on their centre level.; a x b = interaction effect between factor a and b.; a2 = square effect of factor a.; TMMF = total material mass flow rate; L/S ratio = liquid-to-solid mass flow ratio; ScSp = screw speed; Temp.Pre = temperature in the pre-heating zone; Temp.Eva = temperature in the evaporation zone.; (**b**) Square effect of the screw speed on the product LOD. TMMF = 350 g/h, L/S = 0.8, Temp.Pre = 100°C and Temp.Eva = 200°C; (**c**) Pareto plot of significant effects on the process response granules size x_{50}.; (**d**) Interaction effect between the total material mass flow rate and the screw speed on the process response granule size x_{50}.

makes the evaporation zone temperature one of the key parameters for in-barrel-drying. Another possibility of achieving wet granulation combined with drying was indicated at low total material mass flow rate, L/S ratio and screw speed. However, operating in this range would limit the material throughput of the entire manufacturing line.

A crucial process boundary in in-barrel-drying, as in any other drying operation, is the product temperature in relation to the material heat-stability. For drying efficiencies between 40 to 80%, the product temperature was within a range from 55 to 72°C (Fig. 3). When drying was even more efficient, the product temperature increased rapidly. This effect could be explained by the two phases of every drying process, the heat-transfer-limited and the mass-transfer-limited phase (23). In the initial phase of a drying process, heat-transfer limitations are predominant. The material is heated less since energy is consumed by water evaporation. In the following mass-transfer-limited phase, remaining water has to diffuse to the particle surfaces first, before it can evaporate. Therefore, less energy is consumed by water evaporation and subsequently the product temperature increases rapidly. It has to be kept in mind, that the assessed product temperature might not be equal to the highest product temperature in the investigated process, since the granules are rapidly cooled down when exiting the TSG. High product temperatures could trigger significant material degradation and hence impact the product quality. An in-line control is therefore recommended. However, the overall material residence time in the TSG is in the magnitude of a few seconds (24,25) and even shorter in the evaporation zone. Thus, the duration of the high temperature for each particle is extremely short, so the risk of degradation is minimal.

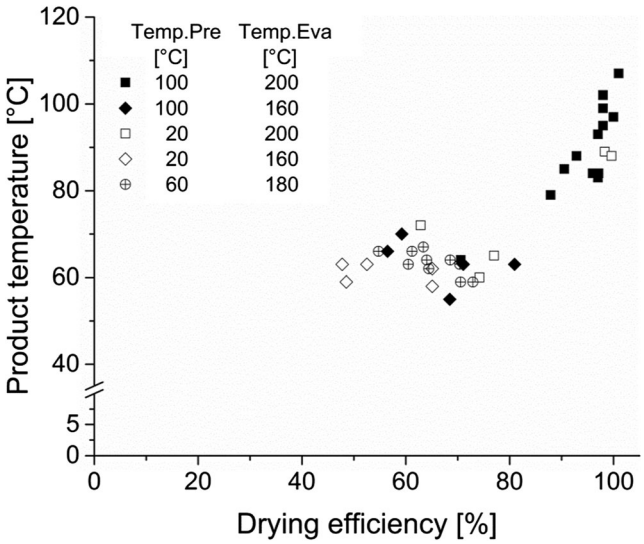

Fig. 3 The product temperature as a function of the drying efficiency. (individual experiments; Temp.Pre = pre-heating zone temperature, Temp.Eva = evaporation zone temperature).

Another fact that has to be considered when interpreting the effects is the confounding of factors that describe the material mass throughput and its composition. The material mass throughput and its composition can be described by the total material mass flow rate, the L/S ratio, the liquid mass flow rate or the solid mass flow rate. However, any two of these factors are enough to describe throughput and composition. Independent from the combination of factors chosen, the factors are confounded in the TSG fill-level, the residence time distribution and/or the processed mass of water. Among other parameters, in a contact dryer the heat-transfer is obviously depending on the contact surface between material and barrel (i.e. the heat-transfer is influenced by the TSG fill-level). Since the liquid, solid and total material mass flow rates are highly confounded in the TSG fill-level, the total material mass flow rate was chosen together with the L/S ratio to describe the material mass throughput and its composition.

Since the L/S ratio and the total material mass flow rate are confounded in the processed mass of water, for example, the drying process as function of the processed mass of water was investigated in more detail. A strong correlation was found for the evaporated mass of water as function of the processed mass of water (Fig. 4a). It was demonstrated, that there was a distinct correlation between the quantity of water processed and the quantity of water that was evaporated (screw speed may have changed simultaneously but had minor effect on this correlation). E.g. at a temperature profile of 100°C in the pre-heating zone and 200°C in the evaporation zone, the evaporated mass of water increased from 84 to 91 g/h to 176 g/h at a processed mass of water of 90 g/h and 250 g/h respectively. This observation can be attributed to an increased contact surface between material and barrel with increasing processed amounts of water. The heat-transfer increases and thereby the evaporated mass of water. But by increasing the processed mass of water, the ratio of the material contact surface with the barrel and the material volume in the TSG becomes less favourable. Only a fraction of the processed mass of water can be evaporated.

Furthermore, it was observed that with increasing barrel zone temperature the evaporated mass of water increased (Fig. 4a). The described small effect of the screw speed on the correlation between the processed and the evaporated mass of water was highlighted especially towards relatively low screw speeds (Fig. 4b). For example, at a processed mass of water of 164 g/h, 60°C pre-heating zone temperature and 180°C evaporation zone temperature, a comparable mass of water was evaporated for the screw speed 200 rpm (99; 101; 104 g/h) and 350 rpm (105 g/h). However, at 50 rpm screw speed the evaporated mass of water was increased to 119 g/h (experiments 11–13 and 18–19). Those findings correspond to the effects that were observed for the process response product LOD. With increasing barrel temperature and decreasing screw speed,

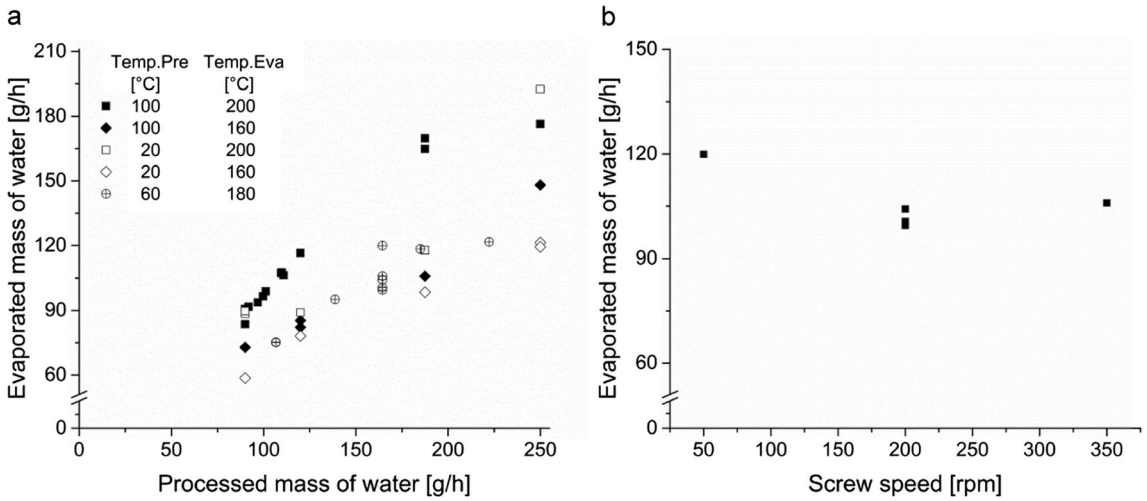

Fig. 4 (**a**) The evaporated mass of water as function of the processed mass of water for various temperature profiles in the barrel zones. The screw speed may have changed simultaneously, but was of minor effect on this correlation. (individual experimental points; Temp.Pre = pre-heating zone temperature; Temp.Eva = evaporation zones temperature); (**b**) The effect of the screw speed on the evaporated mass of water. The temperature profile (Temp.Pre = 60°C, Temp.Eva = 180°C) and the processed mass of water (164 g/h) were kept constant. (individual experimental points).

the product LOD decreased (increasing evaporated mass of water).

A favourable process range, for which completely dried granules were achieved, was found at high barrel zone temperatures and low total material mass flow rate, L/S ratio and screw speed (Fig. 5a). For example, in experiment number 21 the powder blend (LOD = 2.2% *w/w*, x_{10} = 13 µm, x_{50} = 68 µm, x_{90} = 167 µm; (average, n = 3)) was granulated together with 38% *w/w* of water. After in-barrel-drying, the powder blend was found granulated (granule size distribution at x_{10} = 79 µm, x_{50} = 325 µm, x_{90} = 1044 µm) and dried (product LOD = 3.2% *w/w*) (Fig. 5b). Thereby, a drying unit operation downstream of the manufacturing line could possibly be omitted and the material could be tableted directly.

In a next step, the model of the product LOD that was received from the screening DOE was verified for its predictive power by using the optimizer function of the DOE software MODDE. Factor settings were predicted at a confidence interval of 95% for three targeted product LOD values within the evaluated design space for dried granules (Fig. 6a). Although the model suggested a high descriptive and predictive power (R^2 = 0.99; Q^2 = 0.97), two predictions did not match up with the experimental observation. Possible explanations for this deviation could be the relatively low number of performed experiments, the broad knowledge space compared to the narrow design space for dried granules and/or the selection of the model design. The central composite face-centred design may be less susceptible to experimental error

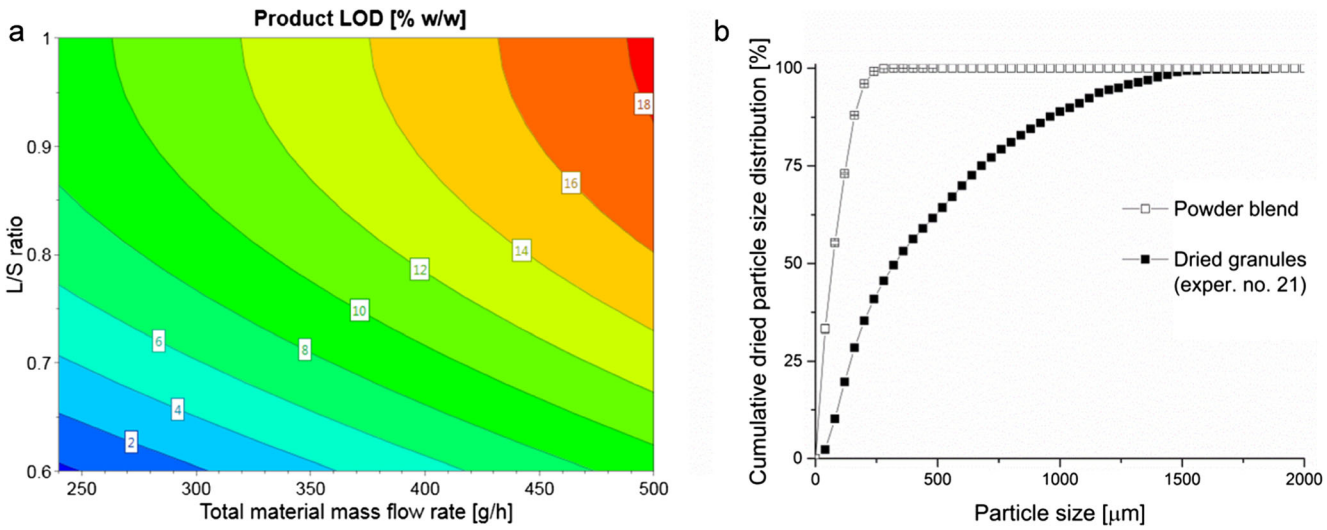

Fig. 5 (**a**) Contour plot of the product LOD for the following factor settings: total material mass flow rate 240–500 g/h, L/S ratio 0.6–1.0, screw speed 80 rpm, temperature in the pre-heating zone 100°C and temperature in the evaporation zone 200°C.; (**b**) The cumulative particle size distribution for the initial powder blend (average ± standard deviation; n = 3), as well as for the granulated and dried material after in-barrel-drying (experiment no. 21; n = 1).

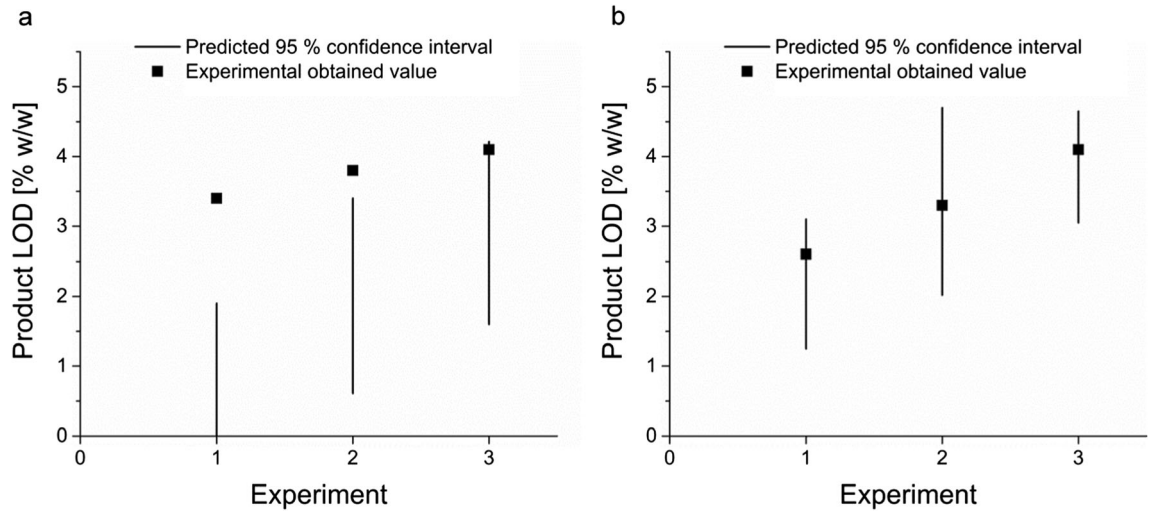

Fig. 6 Predictions for three targeted LOD values at a confidence level of 95% together with the experimental obtained LOD values. (**a**) Screening DOE: for all experiments: pre-heating zone temperature 100°C, evaporation zone temperature 200°C; Experiment 1: total material mass flow rate 287 g/h, L/S ratio 0.62, screw speed 57 rpm; Experiment 2: total material mass flow rate 250 g/h, L/S ratio 0.68, screw speed 60 rpm; Experiment 3: total material mass flow rate 253 g/h, L/S ratio 0.62, screw speed 110 rpm.; (**b**) Optimisation DOE: for all experiments: pre-heating zone temperature 100°C, evaporation zone temperature 215°C; Experiment 1: total material mass flow rate 381 g/h, L/S ratio 0.62, screw speed 47 rpm; Experiment 2: total material mass flow rate 383 g/h, L/S ratio 0.50, screw speed 97 rpm; Experiment 3: total material mass flow rate 392 g/h, L/S ratio 0.65, screw speed 55 rpm.

(all star-points are within the investigated domain). However, such process design provides the operator with lower prediction power at the edges of the domain (in this case the range of interest) and with a basic modelling of quadratic effects only, due to 3 factor levels. Therefore, the learnings of this screening DOE were taken for a follow-up optimisation DOE.

Optimisation DOE

For the optimisation DOE, the factor ranges have been adapted according to the learnings of the first screening DOE (Table IV). The range of the evaporation zone temperature was narrowed and shifted to higher values, extending even the previously investigated knowledge space. The factor range of the pre-heating zone temperature was narrowed to the upper limit of the previously investigated factor range. The factor ranges of the L/S ratio and the screw speed were narrowed to the lower edge of their previously investigated ranges. Since less water was processed (lower L/S ratio) at an increasing material residence time (lower screw speed), higher total material mass flow rates could be targeted. By narrowing the factor ranges, the model resolution was increased. One additional experiment was added to the limit of the domain for extreme conditions (lowest total material mass flow rate, L/S ratio and screw speed combined with highest barrel zone temperatures), to further increase the model resolution in the range of interest. The model design was changed to a central composite circumscribed design, now including 5 factor levels.

After model refinement, models for the product LOD, the evaporated mass of water, the drying efficiency and the product temperature were obtained which displayed high R^2 and Q^2, as well as a high reproducibility (Table V). In contrast, the model that was generated for the granule size x_{50} did not fulfil the criteria of a good model. As outlined for the screening DOE, the relatively low model quality could be explained by the low reproducibility, which in turn could be attributed to the high temperatures in the granulator (the investigated temperature range was higher for the optimisation DOE compared to the screening DOE, which could explain the even lower reproducibility). However, the acceptance range for the granule size x_{50} is typically relative broad since it could be adapted subsequently (e.g. by milling). A poor model fit might therefore be acceptable, as long as the material yielded granulated (granule size x_{50} ranged from 212 to 538 µm and is acceptable). In contrast, the product LOD typically provides a narrow target range. Especially when characterising the in-barrel-drying as a drying process, appropriate models are substantial. Therefore, the focus was put on the drying operation of the in-barrel-drying.

In general, comparable effects were found for the optimisation and the screening DOE. The effect weight had the most significant change. For example, the effect weight of the total material mass flow rate was increased for the process responses in the optimisation DOE, whereas the effect weight of the evaporation zone temperature was decreased. Both can be attributed to the adapted factor ranges that were investigated for the optimisation DOE.

Again, the model that was obtained for the product LOD was verified for its predictive power by using the optimizer function of the DOE software MODDE. Factor settings were predicted at a confidence interval of 95% for three product LOD values within the design space for dried granules (Fig.

Table IV Factor Settings and Obtained Process Responses for the Optimisation DOE

	Factors					Responses				
Exp. Range	TMMF [g/h] 360–560	L/S ratio 0.6–0.8	ScSp [rpm] 50–100	Temp. Pre [°C] 60–100	Temp. Eva [°C] 205–215	ProductLOD [*w/w* %] 2.1–22.9	Evapor. mass H_2O [g/h] 118–201	x_{50} [μm] 212–538	Product temp. [°C] 80–117	Drying efficiency [%] 66–100
1	460	0.7	75	80	200	14.0	152	270	82	80
2	360	0.6	100	60	205	8.8	118	397	91	88
3	360	0.8	50	60	205	10.7	141	495	84	88
4	560	0.6	50	60	205	12.4	169	331	85	80
5	560	0.8	100	60	205	22.9	165	538	83	66
6	360	0.6	50	100	205	3.1	133	225	102	98
7	360	0.8	100	100	205	12.4	136	410	85	85
8	560	0.6	100	100	205	12.6	168	344	84	80
9	560	0.8	50	100	205	15.3	201	349	84	81
10	460	0.7	75	50	210	13.9	152	479	83	81
11	310	0.7	75	80	210	6.7	119	341	99	93
12	460	0.5	75	80	210	4.4	146	212	95	95
13	460	0.7	40	80	210	7.6	173	253	82	91
14 CP	460	0.7	75	80	210	12.5	157	496	84	83
15 CP	460	0.7	75	80	210	12.2	158	334	83	84
16 CP	460	0.7	75	80	210	11.0	163	448	85	86
17 CP	460	0.7	75	80	210	11.4	161	347	85	85
18	460	0.7	110	80	210	13.4	154	302	82	81
19	460	0.9	75	80	210	16.1	177	318	80	81
20	610	0.7	75	80	210	14.1	201	255	82	80
21	460	0.7	75	110	210	10.2	165	451	84	87
22	360	0.6	50	60	215	2.7	134	332	108	99
23	360	0.8	100	60	215	11.6	139	430	87	87
24	560	0.6	100	60	215	11.1	175	333	86	83
25	560	0.8	50	60	215	15.1	201	328	81	81
26	360	0.6	50	100	215	2.1	135	314	117	100
27	360	0.6	100	100	215	6.5	125	435	102	92
28	360	0.8	50	100	215	5.6	153	438	89	95
29	560	0.6	50	100	215	5.4	198	260	92	94
30	560	0.8	100	100	215	17.7	190	433	86	76
31	460	0.7	75	80	220	10.3	165	384	87	87

TMMF total material mass flow rate, *L/S ratio* liquid-to-solid mass flow ratio, *ScSp* screw speed, *Temp. Pre* temperature in the pre-heating zones, *Temp. Eva* temperature in the evaporation zones, *CP* centre point

Table V Summary of Model Fit for the Optimisation DOE after Model Refinement

Process response	Goodness of fit (R^2)	Goodness of prediction (Q^2)	Model validity	Reproducibility
Quality parameters	> 0.50	> 0.50	> 0.25	> 0.50
Product LOD	0.96	0.94	0.71	0.98
Evaporated mass H_2O	0.99	0.97	0.78	0.99
Drying efficiency	0.98	0.96	0.87	0.97
Granule size x_{50}	0.58	0.40	0.95	0.15
Product temp.	0.96	0.88	0.36	0.99

6b). The predictions were aligned with the product LOD that was obtained during the experiments. Thereby the predictive power of the product LOD model from the optimisation DOE was confirmed. The model was then used to predict the process settings for the following investigation of in-barrel-drying and twin-screw wet granulation with API suspension feed.

Combined API Suspension Feed and in-Barrel-Drying

In the final part of this study, in-barrel-drying was investigated for twin-screw wet granulation with API suspension feed. It was evaluated if the previous characterised in-barrel-drying process could indeed be used for reducing or even eliminating separate drying after twin-screw wet granulation. Thereby the in-barrel-drying was compared against the traditional fluidised-bed drying to evaluate the impact of the combined wet granulation and drying process on the product quality in more detail. Granule and compact properties were evaluated.

Indeed, it was found that in-barrel-drying can be used for twin-screw wet granulation with API suspension feed in a single-step operation. As expected, granules were obtained completely dried for the investigated settings. For the traditional wet granulation process, a subsequent drying operation was required (in this study: fluidised-bed drying). For the comparison of both processes, it has to be highlighted that the settings for the screw speed in twin-screw wet granulation were slightly different and that the fluidised-bed drying process was not optimised for this formulation. However, it was found that a drying step could be omitted completely by using in-barrel-drying.

The granule properties were compared. Granules from fluidised-bed drying were found with a significant higher fraction of fines than granules from in-barrel-drying (x_{10} = 38 µm, x_{50} = 85 µm and x_{90} = 494 µm for fluidised-bed drying, compared to x_{10} = 98 µm, x_{50} = 404 µm and x_{90} = 1211 µm for in-barrel-drying (average n = 3)) (Fig. 7a). One explanation could be a higher mechanical stress on the granules during fluidised-bed drying. Another explanation could be the significant difference in the process temperatures in twin-screw wet granulation. In literature it has been described that the solubility of solids in the granulation liquid is of significant impact for the particle agglomeration (26–28). The higher the solubility of solids, the coarser the granules were observed for a similar amount of granulation liquid. For the setup with fluidised-bed drying, twin-screw wet granulation was run at barrel zone temperatures of 20°C, whereas for the in-barrel-drying setup temperatures of around 100°C were applied in the pre-heating and granulation zone. At higher temperatures, the solubility of solids is typically increased (e.g. the solubility of lactose more than doubles, if the temperature is increased from 30 to 60°C (29)). This could have promoted particle agglomeration in in-barrel-drying, compared to the setup with fluidised-bed drying. The bulk density of dried granules from fluidised-bed drying was 0.49 ± 0.01 g/ml and the tapped density was 0.55 ± 0.01 g/ml (average ± standard deviation; n = 3). For granules from the in-barrel-drying process, the bulk density was 0.36 ± 0.01 g/ml and the tapped density was 0.42 ± 0.01 g/ml (average ± standard deviation; n = 3). This can be attributed to the finer particle size of granules from fluidised-bed drying which allows a denser packing with less air entrapment. This can also be visualised by SEM images. The granules from fluidised-bed drying were relatively small in size, whereas the granules from in-barrel-drying were notably coarser (Fig. 7b and c). However, good flowability has been found for granules from both processes (Hausner ratio of 1.14 and 1.15 for fluidised-bed drying and in-barrel-drying, respectively).

The tensile strength of compacts from the fluidised-bed drying was shown to be higher than for the compacts from the in-barrel-drying for compaction pressures up to 150 MPa (Fig. 7d). However, above compaction pressures of 150 MPa, the tensile strength was comparable for both processes. The higher tensile strength of compacts from fluidised-bed drying can be explained by the finer granule size. A denser powder packing (higher tapped density) enables increasing particle-particle bonds, which in turn enhances the tensile strength of subsequent produced compacts (30). The data from the out-of-die porosity supports this argumentation (Fig. 7e). Compacts of granules from fluidised-bed drying were found to be denser with less air entrapment (lower out-of-die porosity) than compacts of granules from in-barrel-drying (for compaction pressures up to 150 MPa). For compaction pressures of 200 MPa or higher, the out-of-die porosity was comparable for both processes, which indicates that the maximum densification of this formulation was reached. The friability of

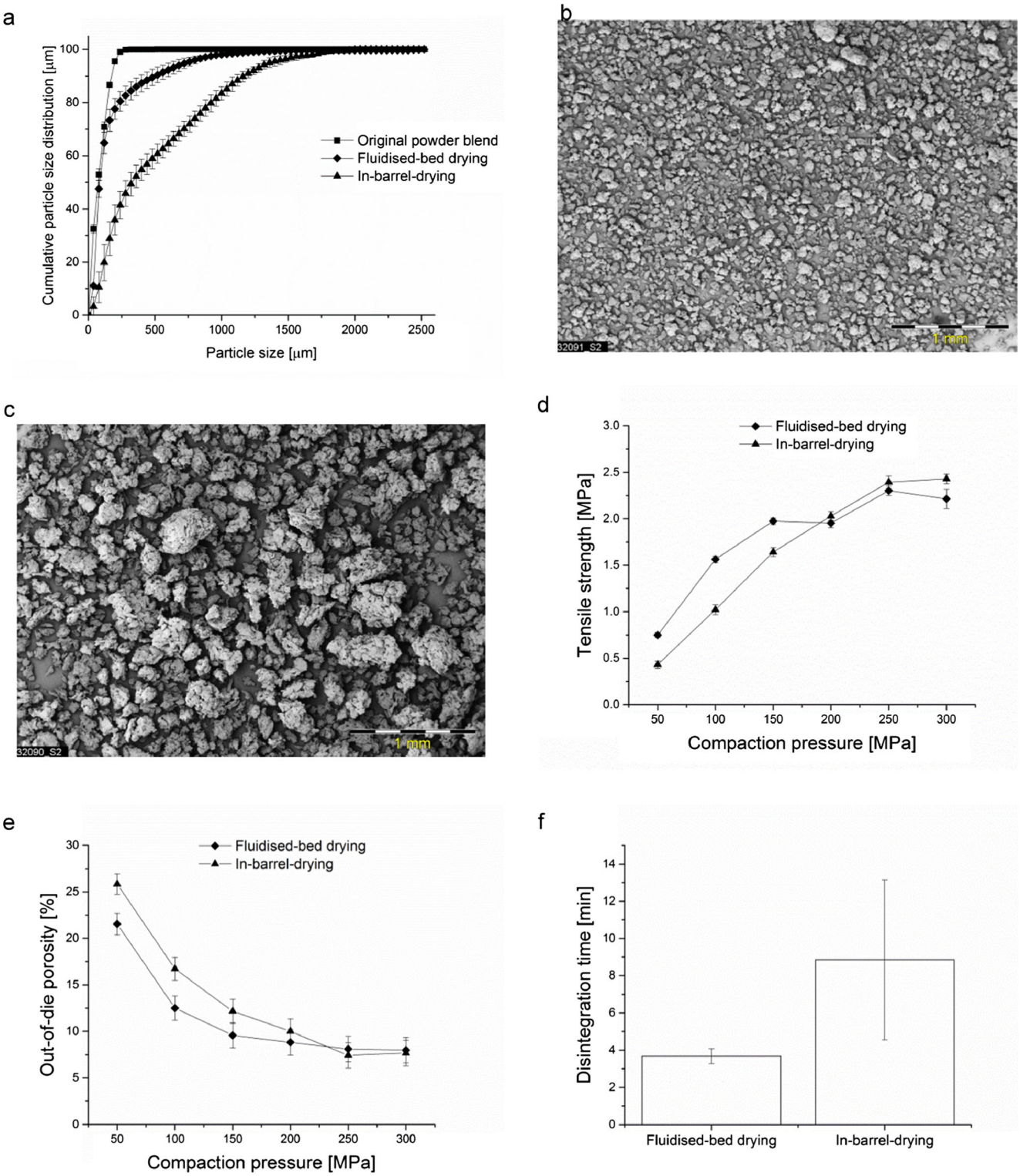

Fig. 7 (**a**) The cumulative particle size distributions of the original powder blend, granules from in-barrel-drying and granules from fluidised-bed drying. (average ± standard deviation; $n = 3$); (**b**) SEM image of granules from fluidised-bed drying.; (**c**) SEM image of granules from in-barrel-drying.; (**d**) The tensile strength as function of the compaction pressure for fluidised-bed drying and in-barrel-drying. (average ± standard deviation; $n = 10$); (**e**) The out-of-die porosity as function of the compaction pressure for fluidised-bed drying and in-barrel-drying. (average ± standard deviation; n = 10); (**f**) The disintegration time of compacts from fluidised-bed drying compared to in-barrel-drying. (average ± standard deviation; $n = 6$).

compacts from all processes was found below 0.4% *w*/*w*, indicating good mechanical stability. Another critical compact property is the disintegration time (Fig. 7f). The disintegration time of compacts from fluidised-bed drying was found to be

three times shorter than for compacts from in-barrel-drying, although the tablet porosity was shown to be lower (fluidised-bed drying: 3:41 ± 0:24 *versus* 8:51 ± 4:18 min:s; average ± standard deviation; $n = 6$; compaction pressure 100 MPa). It is assumed, that the high temperatures during in-barrel-drying could have affected the functionality of the disintegrant sodium carboxymethylcellulose negatively, which is a potential drawback of in-barrel-drying when using Na-CMC as disintegrant. Thereby, the disintegration time, as well as its variability increased for the in-barrel-drying, compared to the fluidised-bed drying. However, material from both processes resulted overall in an acceptable product quality.

CONCLUSION

This study provides an innovative way of combining continuous wet granulation and drying into a single-step process. In-barrel-drying was demonstrated to be feasible and yielded in completely dried and granulated material at specific process settings. Based on these results, a subsequent drying step after twin-screw wet granulation could be omitted in the manufacturing line. The evaporation zone temperature was shown to increase the evaporation capacity of the process without affecting the particle agglomeration. In addition, it was found that the evaporated mass of water increased with an increasing mass of water in the process. However, if completely dried material is targeted, the mass of water that can be evaporated is limited. Hence, the evaporation zone temperature and the processed mass of water were identified as key parameters to balance the evaporation capacity of the process and the material throughput. Another critical aspect observed during the study is the heat-stability of the processed material. The product temperature was shown to increase rapidly towards higher drying efficiencies. This could increase the risk for product degradation and requires careful monitoring of the product temperatures, as well as of degradation products. However, it was found that the in-barrel-drying process can be fine-tuned effectively and controlled by using the screw speed. The screw speed can be adapted instantaneously and gives control over the material residence time and the TSG fill-level (and thereby over the drying efficiency). Furthermore, it was shown that in-barrel-drying can be used together with API suspension feed in the granulation. Granules and compacts from in-barrel-drying with API suspension feed showed significant differences when compared to traditional fluidised-bed drying. A potential drawback of in-barrel-drying may be indicated for the disintegration time when using Na-CMC as a disintegrant. The disintegration time of compacts was shown to be three times longer, compared to compacts from traditional fluidised-bed drying. However, an acceptable product quality was obtained for both processes. It was demonstrated for the first time, that a combination of suspension feeding, granulation and in-barrel-drying can be used to eliminate two separate drying steps in single-step twin-screw wet granulation. However, further efforts are required to generate the understanding to control potential risks (e.g. product degradation or polymorphism if the API is soluble in the suspension liquid and recrystallises during in-barrel-drying) that may come along with that innovative process setup.

ACKNOWLEDGMENTS AND DISCLOSURES.

The authors would like to express their profound gratitude to Mr. Joris Reijneker for the invaluable support to study the in-barrel-drying process as a joint master student.

REFERENCES

1. Crean B, Chen X, Banks SR, Cook WG, Melia CD, Roberts CJ. An investigation into the rheology of pharmaceutical inter-granular material bridges at high shear rates. Pharm Res. 2009;26(5):1101–11.
2. Meier R, Thommes M, Rasenack N, Krumme M, Moll K-P, Kleinebudde P. Simplified formulations with high drug loads for continuous twin-screw granulation. Int J Pharm. 2015;496(1):12–23.
3. van den Ban S, Goodwin DJ. The impact of granule density on tabletting and pharmaceutical product performance. Pharm Res. 2017:1–10.
4. Schmidt A, de Waard H, Moll K-P, Krumme M, Kleinebudde P. Quantitative assessment of mass flow boundaries in continuous twin-screw granulation. Chimia. 2016;70(9):604–9.
5. Rana AS, Hari Kumar S. Manufacturing defects of tablets-a review. JDDT. 2013;3(6):200–6.
6. Amidon GE, Houghton ME. The effect of moisture on the mechanical and powder flow properties of microcrystalline cellulose. Pharm Res. 1995;12(6):923–9.
7. Fonteyne M, Vercruysse J, Díaz DC, Gildemyn D, Vervaet C, Remon JP, et al. Real-time assessment of critical quality attributes of a continuous granulation process. Pharm Dev Technol. 2013;18(1):85–97.
8. Vercruysse J, Córdoba Díaz D, Peeters E, Fonteyne M, Delaet U, Van Assche I, et al. Continuous twin screw granulation: influence of process variables on granule and tablet quality. Eur J Pharm Biopharm. 2012;82(1):205–11.
9. Thompson M, Sun J. Wet granulation in a twin-screw extruder: implications of screw design. J Pharm Sci. 2010;99(4):2090–103.
10. Sayin R, El Hagrasy AS, Litster JD. Distributive mixing elements: towards improved granule attributes from a twin screw granulation process. Chem Eng Sci. 2015;125:165–75.
11. Waje SS, Thorat BN, Mujumdar AS. Screw conveyor dryer: process and equipment design. Dry Technol. 2007;25(1):241–7.
12. Osman HB. Granular flow and heat transfer in a screw conveyor heater: a discrete element modeling study. Master thesis. University of Singapore. 2012.
13. Meena AK, Desai D, Development SAT. Optimization of a wet granulation process at elevated temperature for a poorly compactible drug using twin screw extruder for continuous manufacturing. J Pharm Sci. 2017;106(2):589–600.
14. Seem TC, Rowson NA, Ingram A, Huang Z, Yu S, de Matas M, et al. Twin screw granulation — a literature review. Powder Technol. 2015;276:89–102.

15. Meier R, Moll K-P, Krumme M, Kleinebudde P. Impact of fill-level in twin-screw granulation on critical quality attributes of granules and tablets. Eur J Pharm Biopharm. 2017;115:102–12.
16. Eriksson L, Johansson E, Kettaneh-Wold N, Wikström C, Wold S. Design of experiments: principles and applications. 3rd revised and enlarged edition. Sweden: Umetrics Academy; 2008.
17. Guo Z, Li D, Wang B. A novel concept for convective heat transfer enhancement. Int J Heat Mass Transf. 1998;41(14):2221–5.
18. Kumar A, Vercruysse J, Toiviainen M, Panouillot P-E, Juuti M, Vanhoorne V, et al. Mixing and transport during pharmaceutical twin-screw wet granulation: experimental analysis via chemical imaging. Eur J Pharm Biopharm. 2014;87(2):279–89.
19. Montgomery R. Viscosity and thermal conductivity of air and diffusivity of water vapor in air. J Meteorol. 1947;4(6):193–6.
20. Graves R, Kollie T, McElroy D, Gilchrist K. The thermal conductivity of AISI 304L stainless steel. Int J Thermophys. 1991;12(2):409–15.
21. Iveson SM, Litster JD, Hapgood K, Ennis BJ. Nucleation, growth and breakage phenomena in agitated wet granulation processes: a review. Powder Technol. 2001;117(1–2):3–39.
22. El Hagrasy A, Hennenkamp J, Burke M, Cartwright J, Litster J. Twin screw wet granulation: influence of formulation parameters on granule properties and growth behavior. Powder Technol. 2013;238:108–15.
23. Airaksinen S, Karjalainen M, Räsänen E, Rantanen J, Yliruusi J. Comparison of the effects of two drying methods on polymorphism of theophylline. Int J Pharm. 2004;276(1–2):129–41.
24. Meier R, Thommes M, Rasenack N, Moll KP, Krumme M, Kleinebudde P. Granule size distributions after twin-screw granulation – do not forget the feeding systems. Eur J Pharm Biopharm. 2016;106:59–69.
25. Lee KT, Ingram A, Rowson NA. Twin screw wet granulation: the study of a continuous twin screw granulator using positron emission particle tracking (PEPT) technique. Eur J Pharm Biopharm. 2012;81(3):666–73.
26. Faure A, York P, Rowe RC. Process control and scale-up of pharmaceutical wet granulation processes: a review. Eur J Pharm Biopharm. 2001;52(3):269–77.
27. Lustig-Gustafsson C, Johal HK, Podczeck F, Newton J. The influence of water content and drug solubility on the formulation of pellets by extrusion and spheronisation. Eur J Pharm Sci. 1999;8(2):147–52.
28. Yu S, Reynolds GK, Huang Z, de Matas M, Salman AD. Granulation of increasingly hydrophobic formulations using a twin screw granulator. Int J Pharm. 2014;475(1):82–96.
29. Jelen P, Coulter ST. Effects of supersaturation and temperature on the growth of lactose crystals. J Dairy Sci. 1973;38:1182–5.
30. Sun C, Grant DJW. Effects of initial particle size on the tableting properties of l-lysine monohydrochloride dihydrate powder. Int J Pharm. 2001;215(1–2):221–8.